

Use of a commercial computational fluid dynamics code in the simulation of filtration combustion

Kwang Bo Shim^b, Yong-Chae Chung^b and Sung Chul Yi^a

^aDept. of Chemical Engineering, Hanyang University, Seoul, Korea

^bDept. of Advanced Materials Engineering, Hanyang University, Seoul, Korea

The simulation of combustion phenomena poses a real challenge to numerical methods due to the widely disparate time and length scales present in these systems. Several commercial computational fluid dynamics (CFD) codes with “similar” capabilities in the market are powerful, interactive environment for modeling and solving scientific and engineering problems based on partial differential equations. Some of the processes occurring in real world problems cannot be simulated using the standard version of CFD software. In this study, even though not limited in dimensions, a new two-dimensional model of filtration combustion in FLUENT using user-defined-functions (UDFs) are developed to simulate the self-propagating high-temperature synthesis (SHS) of nitrides.

Key words: SHS, CFD, combustion.

Introduction

The system of governing partial differential equations, together with appropriate initial and boundary conditions, expressing the conservation laws for the transported variables must normally be solved numerically. Analytical techniques as of yet have failed to produce solutions to the full form of the governing equations since the equations describing combustion phenomena are highly nonlinear in nature. It must be mentioned here in passing though that considerable progress in the understanding of combustion has been made possible through the application of analytical mathematical methods employing activation energy asymptotics. As the name itself implies, this particular technique makes the assumption that combustion type reactions can be well approximated in the limit of very large activation energy [1]. A wealth of information and literature has been accumulated over the past decade showing results that are based on the use of activation energy asymptotics. A lot of credit is due to this technique for providing a physical insight into many combustion problems, however simplified in construction they might be. Nevertheless, limitations on the technique clearly exist and to overcome these, one has to resort to numerical solution techniques.

For the application of numerical methods, a number of grid points are distributed over the physical domain or, equivalently, the physical domain is cut up into

many small pieces, called cells. The governing partial differential equations are discretized in one way or the other, resulting in a large system of algebraic difference equations expressing relationships between values of variables at neighboring grid points. Finally, an approximation to the solution of the original partial differential equations is obtained through the solution of this large set of algebraic equations. This is how numerical methods go about finding a solution to a stated physical problem.

Method of Solution Technique

Commercial CFD software has a very versatile solver that can handle many kinds of fluid flow and heat transfer problem. The need for modeling and for solving more and more real world problems with the help of a CFD code determined a strong development of CFD software for various applications and new functions created for niche markets.

Why program in commercial CFD codes? Answers to the question are such that 1) most CFD codes are general-purpose but cannot anticipate all the needs of real world engineering problems, 2) new (physical) models can be developed in a user-friendly environment, and 3) large number of problems (test-cases) can be addressed with the same implementation.

As a result, most commercial CFD codes allow the development of User Defined Functions (UDF) for various applications. Since the core of the software is closed, the newly developed UDFs must be compiled and linked to the main code. Most codes provide macros and additional tools to facilitate the use of UDFs.

*Corresponding author:
Tel : +82-2-2220-0481
Fax: +82-2-2298-5147
E-mail: scyi@hanyang.ac.kr

The UDFs are, in general, either C (Fluent) or FORTRAN (StarCD, CFX) routines programmed by the user linked to the solver to perform certain operations such as 1) initialization, 2) special boundary condition (i.e. space or time dependent), 3) material properties, 4) source terms, 5) reaction rates, 6) post-processing and reporting, and 7) debugging.

In this study, a filtration combustion UDF add-on module of FLUENT code is developed to help the design engineers to analyze and optimize self-propagating high-temperature synthesis (SHS) of nitrides.

A brief description of the UDFs developed in this study is given below.

Description of <filtra.h>

There are a total of two user-defined-scalars (UDSs) and twenty-six user-defined-memory variables (UDMs) defined in this problem.

Description of <filtra-solv.c>

The function *DEFINE_INIT* (*Initialize_Function, domain*) is used for initializing all the user-defined-memory variables (UDMs). This function is called when the problem is initialized in FLUENT.

The function *DEFINE_ADJUST* (*Adjust_Function, domain*) is written to calculate solid phase conversion during transient calculations. This function is called before each iteration.

The function *DEFINE_SOURCE* (*System_pressure_Source, c, t, dS, eqn*) sets the source/sink term in the system pressure equation.

The function *DEFINE_UDS_FLUX* (*UDS_Flux_Condition, f, t, i*) sets convective fluxes of different user-defined-scalars.

The function *DEFINE_UDS_UNSTEADY* (*UDS_Unsteady_Condition, c, t, i, apu, su*) sets transient terms for user-defined-scalars.

Description of <filtra-prop.c>

The function *DEFINE_DIFFUSIVITY* (*Diffusion_Coeff, c, t, i*) computes diffusivity values to be used in the two user-defined-scalar equations.

Description of <filtra-bc.c>

The function *DEFINE_PROFILE* (*Convective_Radiative_UDS1, thread, i*) is used for setting convective and radiative boundary conditions on different boundaries.

Example

The UDFs described above was successfully used for simulation of the filtration combustion process for the synthesis of nitrides. An important subclass of materials prepared by the self-propagating high-temperature synthesis (SHS) is made up of substances that result from the reaction between a porous solid sample and a gaseous reactant. In this way, several hydrides and nitrides have been experimentally obtained [2, 3].

SHS is an efficient method where combustion waves are employed to synthesize the desired high-temper-

ature materials. Using an ignition wire or hot plate, the reactive system is ignited locally. At high temperature, the solid particles react with the gaseous oxidizer to form a solid product. Because the chemical reaction is highly exothermic, it can sustain itself and after a short while the ignition source can be turned off. A luminous region appears, indicating the location of the reaction zone. This zone, under the right conditions, can travel the distance of the system, leaving behind the desired refractory product. The process is self-propagating, meaning no additional external energy needs to be provided. The reader is referred to Dandekar et al. [4] for additional information on the filtration combustion process.

In terms of the dimensionless variables which are standard in the combustion literature [5, 6], the governing equations for a two-dimensional description of the physical system may be written as follows:

mass balance in the gas phase :

$$\frac{\partial(\alpha\bar{\varepsilon}\bar{\rho}_g)}{\partial\bar{t}} - \frac{\partial(\alpha\bar{\varepsilon}\bar{\rho}_g\bar{v}_x)}{\partial\bar{x}} - \frac{\partial(\alpha\bar{\varepsilon}\bar{\rho}_g\bar{v}_y)}{\partial\bar{y}} - \gamma^{-1}R \quad (1)$$

heat balance in the system :

$$\begin{aligned} \frac{\partial(\alpha\delta_1\bar{\varepsilon}\bar{\rho}_g + 1 - \eta + \delta_2\eta)\theta}{\partial\bar{t}} &= \frac{\partial^2\theta}{\partial\bar{x}^2} + \frac{\partial^2\theta}{\partial\bar{y}^2} \\ &- \frac{\partial(\alpha\delta_1\bar{\varepsilon}\bar{\rho}_g\bar{v}_x\theta)}{\partial\bar{x}} - \frac{\partial(\alpha\delta_1\bar{\varepsilon}\bar{\rho}_g\bar{v}_y\theta)}{\partial\bar{y}} + [(1 + \delta_1 - \delta_2)(\beta\gamma)^{-1} + \gamma^{-2}]R \end{aligned} \quad (2)$$

equation of state :

$$\pi = \frac{\bar{p}_g(1 + \beta\theta)}{(1 + \beta\theta_0)} \quad (3)$$

Darcy's law :

$$\bar{v}_x = -\omega \frac{\partial\pi}{\partial\bar{x}} \quad \bar{v}_y = -\omega \frac{\partial\pi}{\partial\bar{y}} \quad (4)$$

reaction rate expression :

$$\frac{\partial\eta}{\partial\bar{t}} = \gamma^{-1}(1 - \eta)\exp\left(\frac{\theta}{1 + \beta\theta}\right)\pi = \gamma^{-1}R \quad (5)$$

The parameters β and γ appear almost everywhere in studies on strongly exothermic reaction systems with a high activation energy. They represent the inverse of the dimensionless activation energy and the inverse of the dimensionless temperature rise, respectively. Parameter α specifies the ratio of the amount of gaseous reactant initially present inside the system to the amount of gas necessary to bring the reaction to full conversion. A low gas pressure therefore corresponds to $\alpha \ll 1$ and high gas pressure to $\alpha \simeq 1$. The permeability of a porous solid structure is measured by parameter ω . When ω is large, the gas velocity will far exceed the reaction front propagation velocity, whereas for a small ω the permeability of the system is very low and the gas mobility is accordingly much less. The heat

capacity ratios are given by δ_1 and δ_2 . For simplicity, it can be assumed that $\delta_2=1+\delta_1$ holds. The form for the dependence of the reaction rate on the conversion was chosen since the reaction rate depends much more strongly on temperature due to the high value of activation energy.

To complete the formulation of the problem, initial and boundary conditions have to be specified in the system. In dimensionless form, they can be written as: the initial conditions :

for $\bar{t}=0$ and $0 \leq \bar{x} \leq \bar{L}_x$, $0 \leq \bar{y} \leq \bar{L}_y$

$$\begin{aligned} \theta &= \theta_o & \eta &= 0 \\ \bar{\rho}_g &= 1 & \pi &= 1 \\ \bar{v}_x &= 0 & \bar{v}_y &= 0 \end{aligned} \quad (6)$$

boundary conditions :

for $\bar{t}_H > \bar{t} > 0$ and

$$\begin{aligned} \bar{x} &= 0 & 0 \leq \bar{y} \leq \bar{L}_y \\ \theta &= \theta_i & \bar{v}_x &= 0 \end{aligned} \quad (7)$$

for $\bar{t} > \bar{t}_H$ and

$$\begin{aligned} \bar{x} &= 0 & 0 \leq \bar{y} \leq \bar{L}_y \\ -\bar{\lambda} \frac{\partial \theta}{\partial \bar{x}} &= \bar{h}_c(\theta - \theta_o) & \bar{v}_x &= 0 \end{aligned} \quad (8)$$

$$\begin{aligned} \bar{x} &= \bar{L}_x & 0 \leq \bar{y} \leq \bar{L}_y \\ -\bar{\lambda} \frac{\partial \theta}{\partial \bar{x}} &= \bar{h}_c(\theta - \theta_o) & \bar{v}_x &= 0 \end{aligned} \quad (9)$$

$$\begin{aligned} 0 \leq \bar{x} \leq \bar{L}_x & & \bar{y} &= 0 \\ -\bar{\lambda} \frac{\partial \theta}{\partial \bar{x}} &= \bar{h}_c(\theta - \theta_o) & \bar{v}_y &= 0 \end{aligned} \quad (10)$$

$$0 \leq \bar{x} \leq \bar{L}_x & & \bar{y} &= \bar{L}_y \\ -\bar{\lambda} \frac{\partial \theta}{\partial \bar{x}} &= \alpha \delta_1 \bar{v}_x [(\bar{\varepsilon} \bar{\rho}_g \theta_o - (\bar{\varepsilon} \bar{\rho}_g \theta)) + \bar{h}_c(\theta - \theta_o) + \bar{h}_r(\theta - \theta_o)] & \pi &= 1 \quad (11)$$

These boundary conditions specify a system with nonadiabatic and convective heat losses from all sides. Radiative heat losses are used only at the top. Ignition by a thermal energy source takes place at $\bar{x}=0$, where the wall is impermeable to gas penetration. The side of the system at $\bar{y}=\bar{L}_y$ is open to the outer atmosphere and the system can thus freely take up a gaseous oxidizer under the right conditions.

In particular, an alternative formulation of the mathematical model is employed which substitutes the mass balance in the gas phase with a pressure evolution equation, obtained through a combination of Eqns. (1), (3), and (4):

$$\frac{\partial \left(\alpha \bar{\varepsilon} \left(\frac{1+\beta \theta_o}{1+\beta \theta} \right) \pi \right)}{\partial \bar{t}} = \nabla \cdot \left(\alpha \bar{\varepsilon} \omega \left(\frac{1+\beta \theta_o}{1+\beta \theta} \right) \pi \nabla \pi \right) - \gamma^{-1} R \quad (12)$$

The system we chose to study is depicted in Fig. 1.

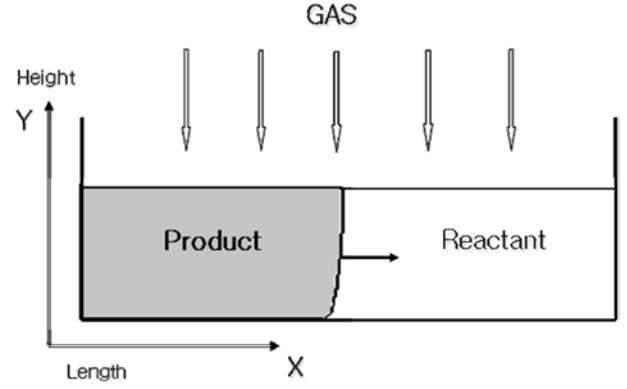


Fig. 1. Cross-flow filtration combustion configuration.

As seen in the figure, gas accessibility to the combustion front is significantly improved in this configuration due to the transport of the gaseous reactant from the surroundings not only by longitudinal flow from the top, but also by transverse flow from regions ahead of the front.

Under a high gas pressure, $\alpha \approx 1$, the amount of gas initially contained inside the porous solid can be sufficient to sustain the combustion process and lead to complete conversion. Although pressure gradients are present, the supply of gaseous oxidizer by filtration is no longer the rate limiting step. Filtration nevertheless still plays an essential role in determining the properties of the product formed and a lot of the combustion process characteristics.

In Fig. 2 contour plots of temperature are shown at different times after ignition. This system is characterized by the dimensionless parameters $\alpha=1.0$, $\beta=0.08$, $\gamma=0.05$, $\delta_1=1.0$, $\delta_2=2.0$, $\omega=30.0$, $\theta_i=0.0$, and $\theta_o=-10.0$. Similar plots are presented for pressure and conversion as well in Figs. 3 and 4, respectively. In Fig. 5 typical carpet plots for temperature and conversion are shown. The velocity vector plot for gas flow is shown in Fig. 6.

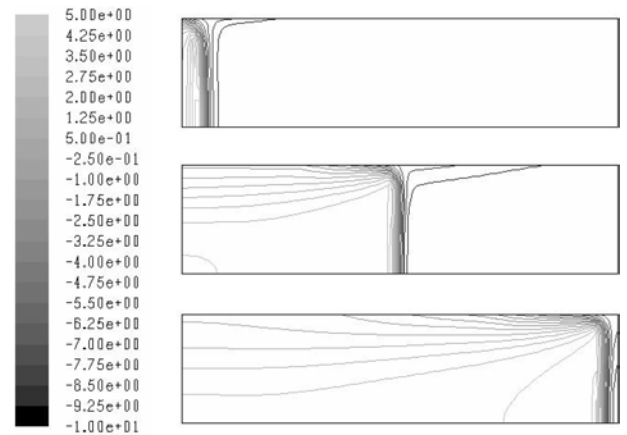


Fig. 2. Combustion front propagation - temperature contours ranging from $\theta=-10.0$ to $\theta=5.0$ in steps of 0.75. Increasing time from top to bottom $\bar{t}=1.4, 7.2, 13.2$.

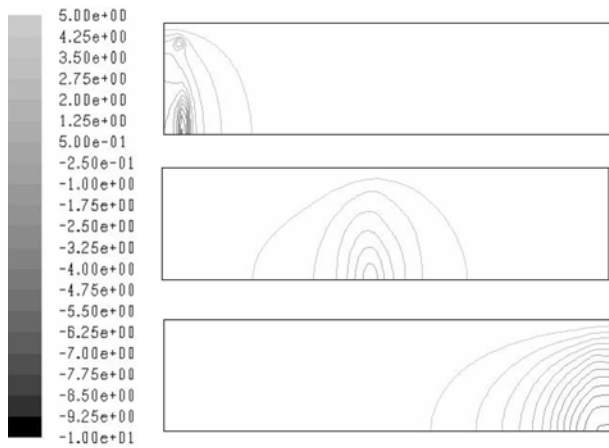


Fig. 3. Combustion front propagation - pressure contours ranging from $\pi=1.0$ to $\pi=0.5$ in steps of 0.025. Increasing time from top to bottom $\bar{t}=1.4, 7.2, 13.2$.

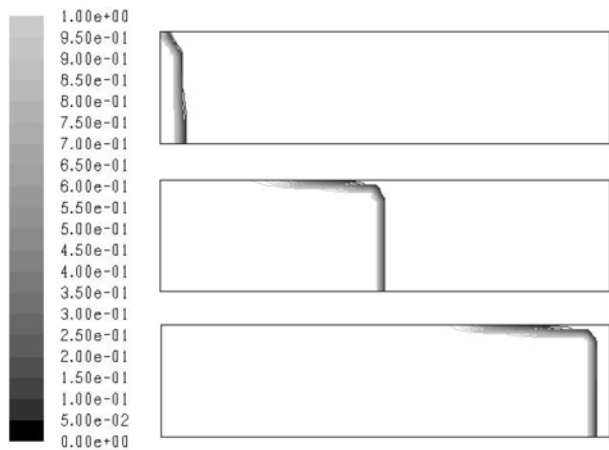


Fig. 4. Combustion front propagation - conversion contours ranging from $\eta=1.0$ to $\eta=0.0$ in steps of 0.05. Increasing time from top to bottom $\bar{t}=1.4, 7.2, 13.2$.

Although this two-dimensional simulation does not provide the full picture, the computational results

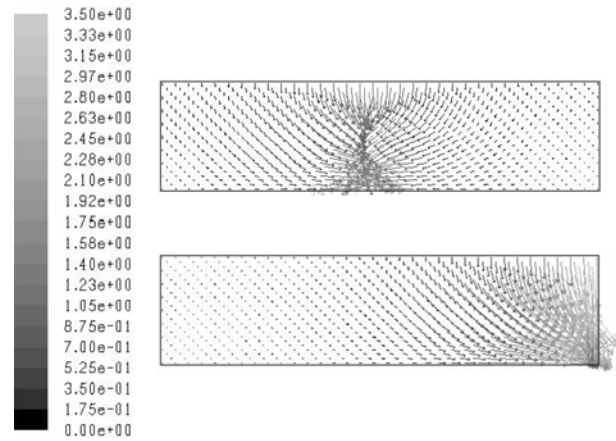


Fig. 5. Gas velocity vector plot at $\bar{t}=7.2, 13.2$.

nevertheless show a striking resemblance to some of the experimental observations. A small perturbation along the reaction front can lead to the formation of hot spots. In experiments, these appear as luminous regions, attesting to the very high temperature present. Because hot spots are very small, localized regions of high temperature, they are required to travel along the reaction front as seen in Fig. 2. The corrugated combustion front uses up the solid reactant in the cold region and also brings in the gaseous reactant ahead of the combustion front as seen in Fig. 6.

Conclusions

It was shown that the FLUENT using user-defined-functions (UDFs) can provide a very powerful tool for the solution of problems involving combustion phenomena. The new two-dimensional model of filtration combustion in FLUENT enhances the capability for design engineers to analyze and optimize the SHS of nitrides.

Even though the model developed in this study is robust, many other changes can be incorporated into

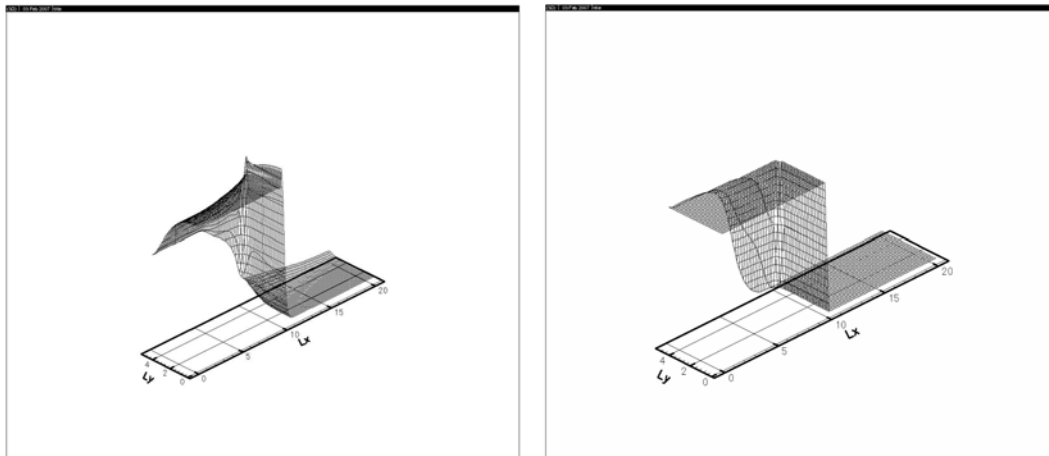


Fig. 6. Three-dimensional carpet plots of temperature and conversion at $\bar{t}=7.2$.

the model as well, such as melting of the solid reactants, chemical reactions occurring in parallel or in series and structural transformations. For filtration combustion, the propagation characteristics of the combustion front due to the addition of an inert gaseous species to the gaseous oxidizer could be considered as well as more accurate representations of fluid flow through a reactive porous medium.

Nomenclature

\bar{L}	: dimensionless length
\bar{h}_c	: dimensionless convective heat transfer coefficient
\bar{h}_r	: dimensionless radiative heat transfer coefficient
\bar{t}	: dimensionless time
\bar{x}, \bar{y}	: dimensionless length coordinate
\bar{v}	: dimensionless velocity
α	: measure of stoichiometric gas amount in void
β	: dimensionless activation energy
γ	: dimensionless heat of reaction
δ	: ratio of specific heats

ε	: void fraction
λ	: effective thermal conductivity
μ	: stoichiometric coefficient
ν	: order of reaction with respect to gas
η	: partial conversion of solid
ω	: dimensionless permeability coefficient
π	: dimensionless pressure
ρ	: density
θ	: dimensionless temperature

References

1. A.P. Aldushin, and Kasparyan, S.G. *Fizika Goreniya i Vzryva* 17 (1990) 37-49.
2. A.G. Aleksanyan, and Dolukhanyan, S.K. *International Journal of Hydrogen Energy* 26 (2001) 429-433.
3. Rosenband, Valery and Alon Gany, *Experimental Thermal and Fluid Science* 31 (2007) 461-467.
4. H.W. Dandekar, Jan A. Puszynski, and Vladimir Hlavacek, *AIChE Journal* 36 (1990) 1649-1660.
5. A.G. Merzhanov, Filonenko, A.K. and I.P. Borovinskaya, *Dokl. Akad. Nauk SSSR* 208 (1973) 122-125.
6. A.D. Merzhanov and Borovinskaya, I.P. *Comb. Sci. Tech.* 10 (1975) 195-211.